

CONCENTRATOR PV INSTALLATIONS BASED ON MODULES WITH FRESNEL MINILENS PARQUETS

V.M.Andreev, V.D.Rumyantsev, N.Yu.Davidyuk, E.A.Ionova, V.R.Larionov,
D.A.Malevskiy, A.O.Monastyrenko, P.V.Pokrovsky, N.A.Sadchikov

Ioffe Physical-Technical Institute, 26 Polytechnicheskaya, 194021, St.Petersburg, Russia
phone: +7-812-2975649, fax: +7-812-2971017, e-mail: vmandreev@mail.ioffe.ru

ABSTRACT: Results of the research and developments in the field of the terrestrial PV modules and installations realizing the concept of very high sunlight concentration by the use of composite glass-silicone Fresnel lenses and multijunction III-V solar cells (SCs) are described. The main components for a high-concentration PV (HCPV) concept have been developed: panels of small-aperture Fresnel lenses; reflective and refractive secondary optical elements; triple-junction cell strings with passive heat spreaders; “carousel” and “tower”-type tracker in the range of 1-5 kWp of installed power. Composite glass-silicone Fresnel lenses 40 x 40 and 60 x 60 mm² in size (plan view) with focal lengths of 70 and 110 mm, respectively, are used as primary concentrators. The focal length of secondary plane-convex glass lenses is varied from 5 to 25 mm. With the shortest-focal-length secondary lenses used, measurements of parameters of the photovoltaic converter in a system with radiation concentrators with pulsed solar testers show the increase in the concentration ratio and the expansion of the misorientation curve by a factor of 2.5–3.0. The parameters of the test modules with lens panels measured under solar illumination are found to be in a good agreement with laboratory data. For 0.5x0.5 m² concentrator modules, overall conversion efficiency is in the range of 26-27% at cell efficiency 35-36%. The concentrator modules are arranged on sun trackers with a programmable/analog sun positioning mechanism. Serial production of the high-efficient and low-cost solar concentrator PV installations is in progress, being aimed to achieve the production capacity of 100 MW/year.
Keywords: solar cell, concentrator, PV installation

1 INTRODUCTION

Solar energy conversion by means of high efficient nanoheterostructure III–V solar cells seems to be one of the most promising approaches for reduction of the solar electricity cost [1-4]. The economic effect of using such SCs is provided owing to cheap sunlight concentrators.

The composite Fresnel lens design, in which the front region is a sheet of normal silicate glass, the inner surface serving as a substrate accommodating a concentric set of refractive microlenses made of a transparent silicone compound, is today viewed as promising one [5, 6]. Since the rise in the sunlight concentration ratio is intimately related to saving the area occupied by semiconductor chips, the rise in the ratio averaged over the chip’s surface area reduces the partial SC cost in the total cost of unit power from a solar plant. Remind that the SC operation at a high photocurrent density is also preferable when it comes to achieving ultimate efficiency [7].

For the conversion of concentrated solar radiation to be efficient, a mechanical sun tracking by the “concentrator–SC” system is necessary. The higher the concentration ratio, the higher must be the tracking accuracy. However, one can constrict the solar spot on the SC surface by increasing locally the concentration ratio and thereby allowing the displacement of the spot within the light-sensitive area without decreasing the output power. In this way, the range of allowed solar module misorientation angles can be extended, and the requirements on the tracking accuracy can be reduced. Thus, the SC operation at a high light flux density is desirable as far as the physics of the process and the design of photovoltaic systems are concerned.

It should be noted that the sunlight concentration ratio in a “concentrator–SC” system is limited. Limitations depend on the focusing force of Fresnel

lenses and on the capability of the SC design to minimize the internal electrical resistance and withstand thermal loads. A secondary optical element added to the optical scheme of a photovoltaic system may considerably improve its performance. Usually, conic reflectors are used as secondary elements. They are made of polished aluminum sheet or glass block with polished lateral surfaces [8–10]. In the latter case, the effect of total internal reflection at the glass–air interface is used. The disadvantage of conic reflectors is the need to mount them in the vicinity of the SC: by providing a very narrow gap in the case of hollow aluminum reflectors or an optical contact (using an appropriate adhesive compound) in the case of glass reflectors.

One can apply small plane-convex lenses as secondary optical elements. Such lenses, placed at a distance from the SC surface, focus the radiation from the primary Fresnel lens [5, 10]. One of the aims of this work is gaining a deep insight into the effect of secondary lens concentrators on the output parameters of solar modules including primary Fresnel lenses and efficient triple-junction SCs.

2 DESIGN OF CONCENTRATOR SOLAR MODULES

The concentrator module is made in the form of a front lens panel connected to a rear energy-generating panel with aluminum walls. The panels are the focal distance of the lenses apart. The lens panel represents a sheet of silicate glass with small-size Fresnel lenses right up to each other on its inner surface. The Fresnel lenses are made of a silicone compound.

Figure 1 shows the part of a unit module in which composite Fresnel lenses and a small plane-convex lens serve as primary concentrators and a secondary

concentrator, respectively. A SC is mounted on a copper heatsink, which, in turn, is placed on the outer surface of the rear glass base of the module. To protect the module against environmental action, a thin air gap between the shaped heat-spreading plate and the glass base is sealed. The small plane-convex lens is glued on the inner surface of the rear base of the module in front of the SC. The composite glass–silicone Fresnel lenses have a square shape measuring in plan view either $40 \times 40 \text{ mm}^2$ (hereinafter FL40) or $60 \times 60 \text{ mm}^2$ (FL60). Focal length F of the primary lenses measured from the inner surface of their glass substrate was equal to 70 and 110 mm, respectively. The diameter of the photosensitive area of the SC equaled to 1.7 mm for the smaller lenses and 2.3 mm for the larger ones.

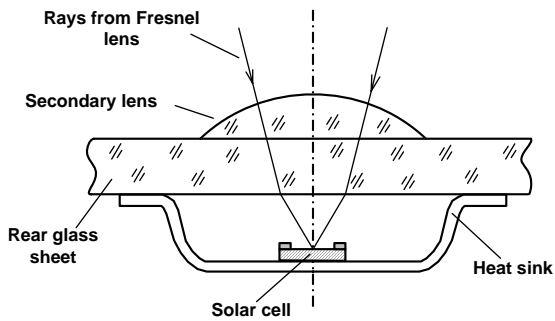


Figure 1: Design of the submodule with secondary optical element.

In laboratory experiments using a solar tester, focal length f of the secondary plane-convex glass lens was varied from 5 to 25 mm and distance h between the front and rear bases of the module was varied with an adjustment gear on a mechanical support. From the results of these experiments, we prepared unit and multiple-Fresnel-lens test modules intended for field tests under solar illumination.

3 MEASURING PROCEDURE

Laboratory experiments with unit concentration modules were conducted using the original solar tester comprising a pulsed light source (xenon lamp), a collimator, and a measuring block [11]. The tubular glowing region of the lamp was covered by a light-impermeable shield with a hole 6 mm in diameter. The hole was at the focal point of an aberration-free reflecting objective. The focal distance of the objective was larger than the diameter of the hole 100-fold, so that the residual divergence of the collimated radiation corresponded to the divergence of sun rays ($32'$). The radiation spectrum of the lamp was corrected by an interference filter so as to meet the AM 1.5 solar spectrum.

The power density of the pulsed radiation having passed through the collimator was set equal to 850 W/cm^2 . The concentrator photovoltaic system (Fresnel lens–secondary lens–SC with heatsink) was mounted on mechanical adjustment gears making it possible to align the elements, control the distance between them, and provide transverse rotation of the whole system about the optical axis of the collimator.

A triple-junction InGaP/GaAs/Ge SC was soldered to the shaped heat-spreading plate, which, in turn, was mounted in the immediate vicinity of the rear glass base of the module with a 0.5-mm gap between the glass and SC. The SC was connected to the measuring unit of the tester. The power supply of the lamp, measuring unit, and mechanical gears were controlled with a computer.

The xenon lamp generated 1-ms-long flat light pulses. Within the flat part of the pulse, a sweep voltage was applied to the SC to take an illuminated I – V characteristic. A data acquisition system recorded the parameters of the I – V curve, such as the short-circuit current (I_{sc}), output power at the optimal illuminated point (P_{max}), fill factor (FF) of the characteristic, and photovoltaic conversion efficiency. In a number of experiments, a misorientation curve of the module, that is, the dependence of the current I_{sc} on the angle between the optical axes of the module and collimator, was constructed. The permissible range of the radiation acceptance angle was estimated from the half-width of this curve at a level of $0.9 (\pm W_{0.9})$ under normal incidence of sun rays on the primary lens. Also, we made photometric measurements of the light spot on the SC surface. To do this, the SC was replaced by a single-junction GaAs photodetector with an aperture 0.12 mm in diameter. Special calibration allowed us to determine the absolute value of the local radiation concentration ratio and estimate the diameter of the spot from the value of 0.1 of the maximal photocurrent at the center ($d_{0.1}$).

The photovoltaic parameters of the test modules under field conditions were measured with the modules placed on the sun-tracking system. Load I – V curves were recorded using an analog-to-digital measuring unit, and the power density of direct solar radiation was measured with a Kipp and Zoned CH-1 calibrated pyrheliometer and a solar cell calibrated in the National Renewable Energy Laboratory (Golden, Colorado, United States).

4 RESULTS OF LABORATORY EXPERIMENTS

At the first stage of investigation, we selected optimal distance h for each pair of primary and secondary lenses (taken from a prepared set, see below) incorporated into a module. As the optimization criterion, we chose maximization of the photovoltaic conversion efficiency (note that the efficiency may both increase with varying distance because of better focusing and decrease because of a too high local concentration of radiation, which causes the FF in the illuminated I – V curve to decrease).

By way of example, Fig. 2 plots I_{sc} , FF, and efficiency (Eff) versus distance h for an FL60 and a SC 2.3 mm in diameter. This figure also gives us an idea of the necessary accuracy of primary and secondary lens arrangement along the optical axis (this accuracy equals 0.25 mm).

The parameters I_{sc} , P_{max} , Eff , C_{max} , and $\pm W_{0.9}$ of the test unit modules measured under laboratory conditions with the solar tester. The following features are typical of the modules of both sizes: FL40 and FL60. As expected, an intermediate rear glass introduced into the arrangement of secondary lenses reduces the current and efficiency as a result of light reflection at two additional glass–air interfaces. The introduction of long-focus secondary lenses with a one-sided antireflection coating

raises the current through a partial decrease in the reflection and a better collection of the light on the SC surface.

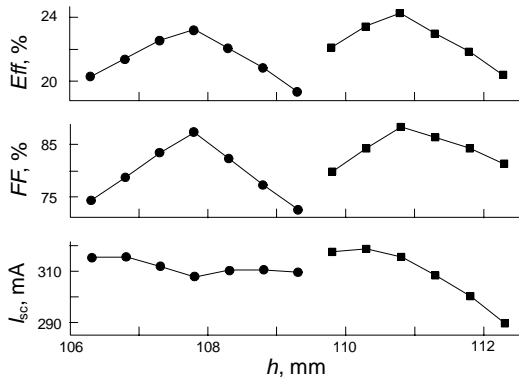


Figure 2: I_{sc} , FF, and conversion efficiency vs. distance h for an FL60 in combination with the SC 2.3 mm in diameter. The curves on the right are depicted for the case when secondary optical elements are absent, and those on the left refer to the case when a secondary lens with focal length $f = 8$ mm is introduced.

In the case of short-focus secondary lenses, the current to a great extent recovers even in the absence of antireflection coatings. This takes place outright thanks to focusing of the radiation. A positive fact here is that the FF of the I - V curve was always higher than 85% despite the considerable decrease in the light spot diameter and its corresponding increase in the local concentration ratio of radiation.

When the optical axis of the module is offset from the axis of the radiation source, a smaller light spot may stay on the SC surface for a longer time. That is why the misorientation characteristic of the modules expands threefold in the case of the shortest-focal-length lenses. From Fig. 3,4,5, it follows that the set of parameters of secondary lenses with $f = 8$ mm is optimal for application in the modules of both sizes.

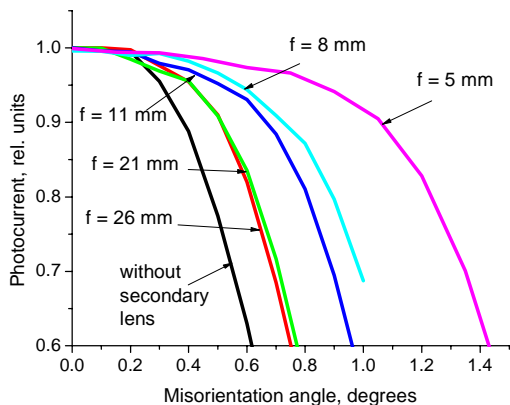


Figure 3: The results on misorientation angle measurements for a PV sub-module with 40x40 mm² primary Fresnel lens, a solar cell 1.7 mm in diameter and secondary lenses of different focal distances f .

At misorientating the submodule axis, a light spot of smaller diameter can remain for a longer time on the SC

surface. In Figure 3, the results on misorientation angle measurements are presented for a sub-module with a primary Fresnel lens of 40x40 mm², solar cell 1.7 mm in diameter and secondary lenses of different focal distances f . The data are in arbitrary units for better comparison of the curves.

In Figure 4, the similar results are presented for the case of a cell 2.3 mm in diameter. Widening the contours of the module misorientation characteristics almost in three times in the case of the shortest-focus secondary lenses was observed.

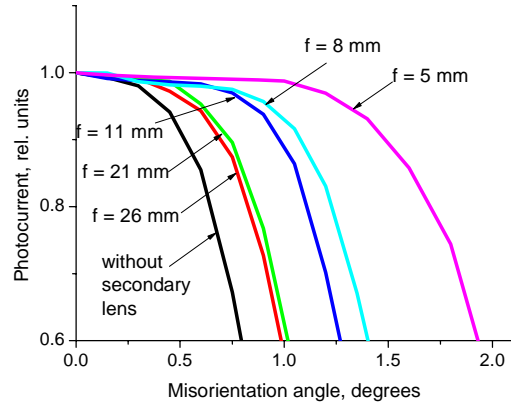


Figure 4: The results on misorientation angle measurements for a PV sub-module with a 40x40 mm² primary Fresnel lens, a solar cell 2.3 mm in diameter and secondary lenses of different focal distances f .

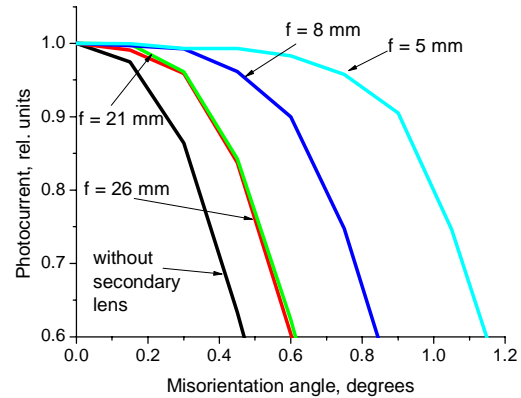


Figure 5: Photocurrent vs tilt angle for sub-modules based on 60 mm x 60 mm Fresnel lens with convex secondary lenses of different focal distances and $d_a = 2.3$ mm.

In Figure 5, the similar results are presented for the sub-module based on 60 x 60 mm² Fresnel lens and cell diameter of 2.3 mm. Misorientation angle $W_{0.9} = \pm 0.6$ angular degree at $f = 8$ mm and $W_{0.9} = \pm 0.9$ angular degree at $f = 5$ mm.

Figure 6 (curves 1,2) shows the summary of the results presented in Fig. 3,5 and curves 3,4 demonstrate the increase of the maximum local sunlight concentration (C_{max}) with the decrease of focal distance of secondary lens. At optimum $f = 8$ mm, C_{max} exceeding 4000x. The additional cylindrical glass kaleidoscope in the design shown in Fig. 11 ensures the uniformity of solar cell illumination without reducing the misorientation angle. Diameter of this kaleidoscope is equal to cell diameter.

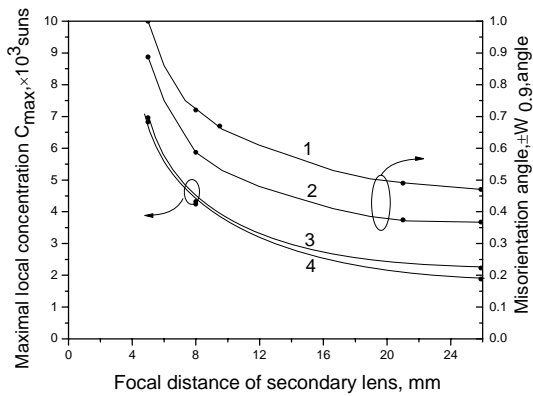


Figure 6: Misorientation angle ($\pm W_{0.9}$, curves 1,2) and maximum local sunlight concentration (C_{max} , curves 3,4) vs. focal distance of secondary lenses for two PV submodules: curves 1,4 – submodule with $40 \times 40 \text{ mm}^2$ Fresnel lens and solar cell diameter $d_a = 1.7 \text{ mm}$, curves 2,3 – $60 \times 60 \text{ mm}^2$ Fresnel lens and $d_a = 2.3 \text{ mm}$.

5 RESULTS OF OUTDOOR TESTING

Field measurements under solar illumination were made for unit and multilens concentrator modules without secondary lenses (reference modules) and for modules with secondary lenses (focal length $f = 8 \text{ mm}$). Figure 7 shows the load $I-V$ curves of the unit module with FL40 and the SC 1.7 mm in diameter under illumination by sun rays incident normally to the front surface of the module. The dashed line refers to the module without the secondary lens. Since this module incorporates the best examples of the primary Fresnel lens and SC, its efficiency is as high as 27.1%. The solid curve in Fig. 7 refers to the case when the secondary lens with $f = 8 \text{ mm}$ is introduced. Here, the efficiency is somewhat lower, 25.7%. The decrease in the efficiency by 1.4% is due to the reflection from two additional glass faces. It can be completely compensated for with the help of antireflection coatings.

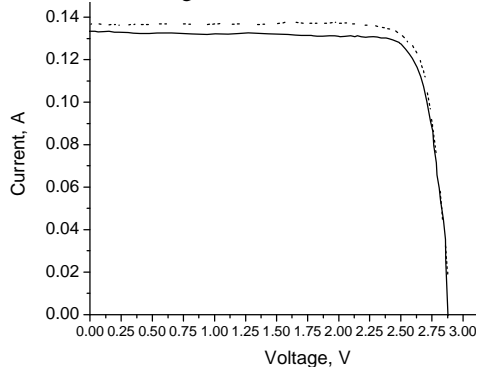


Figure 7: Illuminated $I-V$ curves of the unit module with the FL40 and SC 1.7 mm in diameter under solar illumination. The dashed line refers to the case when the secondary lens is absent, power density E of incident solar radiation is 786 W/cm^2 , and the efficiency of the module is 27.1%. The solid curve refers to the case when the secondary lens with $f = 8 \text{ mm}$ is introduced, $E = 790 \text{ W/cm}^2$, and the efficiency of the module is 25.7%. The ambient temperature is 22°C . The values of the efficiency are not corrected to the increased temperature of the SC.

Figure 8 demonstrates misorientation curves (the dependences of the short-circuit current on the angle between the optical axis of the module and the direction toward the Sun) for the same module with and without the secondary lens. The secondary lens is seen to increase the width of the curve at a level of 0.9, $\pm W_{0.9}$, from $\pm 0.39^\circ$ to $\pm 0.72^\circ$.

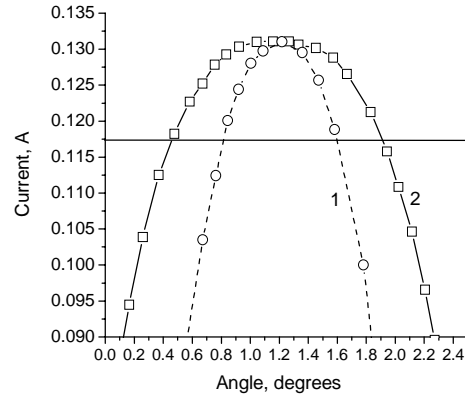


Figure 8: Misorientation curves for the FL40-based module with the SC 1.7 mm in diameter under solar illumination (I) without the secondary lens, $\pm W_{0.9} = \pm 0.39^\circ$, and (2) with the secondary lens ($f = 8 \text{ mm}$), $\pm W_{0.9} = \pm 0.72^\circ$.

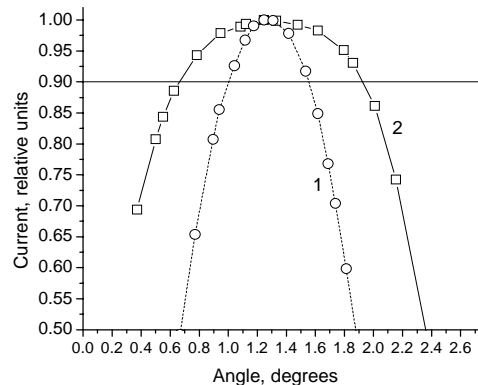


Figure 9: Misorientation curves under solar illumination for two eight-lens modules with FL60 and SC 2.3 mm in diameter (I) without secondary lenses ($\pm W_{0.9} = \pm 0.27^\circ$) and (2) with secondary lenses with $f = 8 \text{ mm}$ ($\pm W_{0.9} = \pm 0.64^\circ$).

Figure 9 demonstrates the misorientation curves for FL60 module with $60 \times 60 \text{ mm}^2$ Fresnel lenses and solar cell diameter of 2.3 mm.

6 SUN TRACKERS AND PV INSTALLATIONS

The concentrator modules are mounted on the sun trackers. Two types of trackers are under development – of “carousel” design and of “tower” design (see pictures in Fig.10). A range of nominal output power of the solar installations is 1–5 kWp for “tower”-type trackers and 1.0 kWp for “carousel” ones. Each tracker is equipped with analog sun sensor for positioning the frame with modules in direction to the Sun with accuracy of about 0.1 degree of arc. Also, there exists a digital circuit for

programmable rotation of the trackers from sunset to sunrise position and during cloudy periods.

The installations in Fig. 10 contain 18 modules, which ensure 1 kWp of output power.

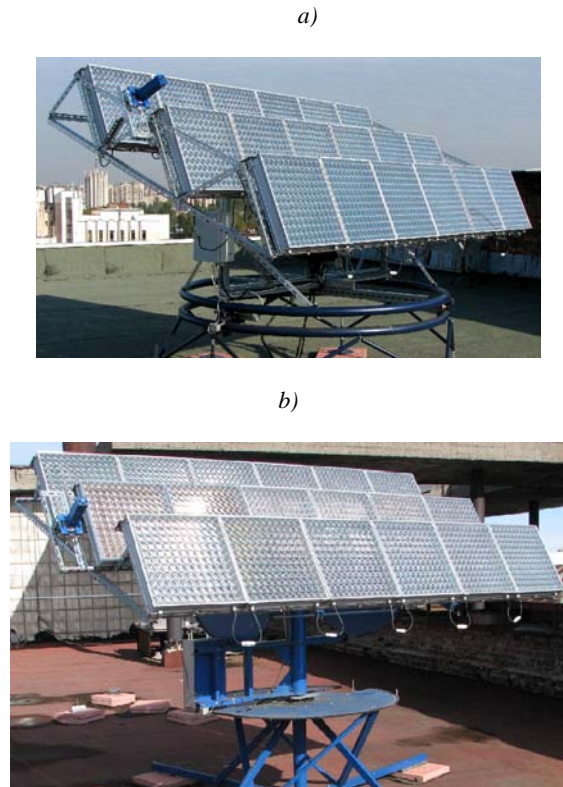


Figure 10: a) PV installation with “carousel”-type tracker and concentrator modules for 1 kWp of output power. b) PV installation with “tower”-type tracker.

7 ORGANIZING THE PRODUCTION OF SOLAR INSTALLATIONS WITH CONCENTRATORS

Original design and the fabrication methods of SC chips, Fresnel lenses, secondary concentrators, photoreceiver plates, concentrator PV modules, sun trackers and PV systems are protected by 33 patents and applications for patents.

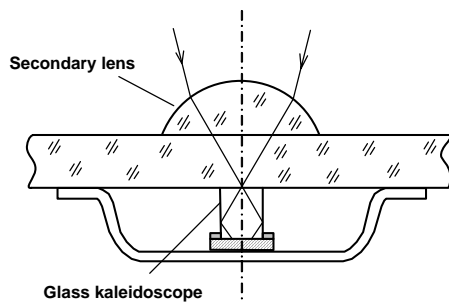


Figure 11: Design of submodule with “short focus” convex lens and with additional kaleidoscope, glued on the cells surface.

For production goals, new module design based on “short-focus” secondary lens and additional glass kaleidoscope (Fig. 11) has been developed to provide the uniformity of SC illumination at misorientation angle $\pm W_{0.9}$ exceeding ± 1 angle degree.

Additional improvement of module design has been made by increasing the module dimensions to $0.5 \times 1 \text{ m}^2$ (Fig. 12), that should decrease the specific cost of installed power at high scale production.



Figure 12: CPV module with dimensions of $0.5 \times 1 \text{ m}^2$ based on 288 submodules of $4 \times 4 \text{ cm}^2$ each.

Assumed technical parameters for industrial production are the following: - application of solar cells with the efficiency of up to 38% for concentrated sunlight conversion; - sunlight concentration up to 1000x by means of Fresnel lenses with optical efficiency as high as 87%, resulting in decrease of the solar cell area and its specific cost; - increasing the module dimensions to $0.5 \times 1 \text{ m}^2$; - increasing the specific power output up to 250 W/m^2 ; - sun tracking by means of two-ax systems with an accuracy of ± 0.1 angle degree; - increasing the amount of electric power generated from the CPV array specific area in more than 2 times compared to the stationary silicon solar arrays.

Enumerated tasks require solving the problems connected with adjustment of the existent industrial equipment to the purposes of the concentrator PV. Also, there are the problems of creation of a new specialized equipment. For instance, flash solar tester for in-line output certification of the assembled concentrator modules is needed. In Fig. 13, a newly developed at PV Lab solar tester is shown for I-V measurements of the advanced concentrator modules with aperture area up to $0.5 \times 1 \text{ m}^2$. Illumination system of this tester forms collimated light flux with divergence of $32'$ at 1 sun intensity and spectrum corresponding to AM 1.5d. Measurement productivity of the tester is 250 I-V curves per hour.

The new sun tracker (Fig. 14) providing the output power of 5 kW_p has been created for serial production. The modules are connected with a full-scale “controller-battery-inverter” system. Also, there is a computerized acquisition system, allowing the periodic measurements of the I-V curves in a representative set of the modules.



Figure 13: Flash solar tester for I-V measurements of the advanced concentrator modules with aperture area up to $0.5 \times 1 \text{ m}^2$ (shown as well). Collimated light flux with divergence of $32'$ at 1 sun intensity and spectrum corresponding to AM 1.5d is generated by four flash lamps.



Figure 14: PV installation, which ensure appr. 5 kWp of output power (two lower rows – the concentrator modules; three upper rows – commercially available Si-based flat-plate modules).

Production planning includes two stages: - production of nanoheterostructures, solar cells, concentrator photovoltaic modules and installations with the total prescribed power of 10 MW/year; - serial production of cells, modules and installations with the total power of more than 85 MW/year.

The Russian Corporation of Nanotechnologies (RUSNANO) is the main investor for this project. The priority of RUSNANO is commercialization of nanotechnology projects with high business potential and/or social benefit. Its financial contribution in early-stage technology companies reduces risks of private investors. Corporation holds a minority share (under 50%) leaving the rest of the share to founders and private capital in order to ensure that the project is realized with maximum efficiency.

8 CONCLUSION

Main R&D activity on HCPV with III-V-based solar cells is centered at the Ioffe Physical-Technical Institute. Basic components of the HCPV facilities are under development: 3-junction cells, panels of the Fresnel lenses; secondary optical elements; cell strings and modules; sun tracking systems and concentrator PV installations of different design for nominal power in the range of 1–5 kWp. Current stage of work assumes commercialization of the HCPV product.

9 ACKNOWLEDGMENTS

This work was supported by the Russian Foundation for Basic Research, grants no. 09-08-00412 and no. 09-08-12202.

10 REFERENCES

- [1] Zh.I.Alferov, V.M.Andreev, and V.D.Rumyantsev, *Fiz. Tekh. Poluprovodn.* (St. Petersburg) **38**, 937 (2004) [*Semiconductors* **38**, 899 (2004)].
- [2] Zh.I.Alferov, V.M.Andreev, and V.D.Rumyantsev, *High-Efficient Low-Cost Photovoltaics*, Springer Ser. Opt. Sci. **140**, 101 (2008).
- [3] N.H.Karam, R.A.Sherif, and R.R.King, *High-Efficient Low-Cost Photovoltaics*, Springer Ser. Opt. Sci. **140**, 199 (2008).
- [4] A.W.Bett, F.Dimroth, and G.Siefer, *High-Efficient Low-Cost Photovoltaics*, Springer Ser. Opt. Sci. **140**, 67 (2008).
- [5] V.D.Rumyantsev, O.I.Chosta, V.A.Grilikhes, N.A.Sadchikov, A.A.Soluyanov, M.Z.Shvarts, and V.M.Andreev, in *Proceedings of the 29th IEEE Photovoltaic Specialists Conference (PVSC)*, 2002, New Orleans, pp. 1596–1599.
- [6] V.D.Rumyantsev, *Concentrator Photovoltaics*, Springer Ser. Opt. Sci. **130**, 151 (2007).
- [7] V.M.Andreev, V.A.Grilikhes, and V.D.Rumyantsev, *Photovoltaic Conversion of Concentrated Solar Radiation* (Nauka, Leningrad, 1989) [in Russian].
- [8] K.Araki, M.Kondo, H.Uozumi, and M.Yamaguchi, in *Proceedings of the 3rd World Conference on Photovoltaic and Energy Conversion*, Osaka, 2003, pp. 853–856.
- [9] J.Jaus, P.Nitz, G.Peharz, G.Siefer, T.Schult, O.Wolf, M.Passig, T.Gandy, and A.W.Bett, in *Proceedings of the 33rd IEEE Photovoltaic Specialists Conference*, San Diego, 2008.
- [10] V.D.Rumyantsev, N.Yu.Davidyuk, E.A.Ionova, V.R.Larionov, D.A.Malevskiy, P.V.Pokrovskiy, N.A.Sadchikov, and V.M.Andreev, in *Proceedings of the 5th International Conference on Solar Concentrators for the Generation of Electricity*, Palm Desert, 2008 (Proceedings on CD).
- [11] V.M.Andreev, V.R.Larionov, I.V.Lovygin, D.A.Malevskii, M.Ya.Maslenkov, V.D.Rumyantsev, and M.Z.Shvarts, in *Proceedings of the International Forum on Nanotechnology*, Moscow, 2008, Vol. 1, pp. 205–207.